



## Geology of the lower Belice River valley, epicentral area of the $M > 5$ 1968 seismic sequence (south-western Sicily, Italy)

Stefano Pucci, Giuseppe Avellone, Antonio Contino, Alessandro Incarbona, Leonardo Sagnotti, Attilio Sulli, Enrico Di Stefano, Alessandra Smedile, Anna Maria Gueli & Giuseppe Stella

To cite this article: Stefano Pucci, Giuseppe Avellone, Antonio Contino, Alessandro Incarbona, Leonardo Sagnotti, Attilio Sulli, Enrico Di Stefano, Alessandra Smedile, Anna Maria Gueli & Giuseppe Stella (2023) Geology of the lower Belice River valley, epicentral area of the  $M > 5$  1968 seismic sequence (south-western Sicily, Italy), Journal of Maps, 19:1, 2242725, DOI: [10.1080/17445647.2023.2242725](https://doi.org/10.1080/17445647.2023.2242725)

To link to this article: <https://doi.org/10.1080/17445647.2023.2242725>



© 2023 The Author(s). Published by Informa UK Limited, trading as Taylor & Francis Group on behalf of Journal of Maps



[View supplementary material](#)



Published online: 08 Aug 2023.



[Submit your article to this journal](#)



Article views: 578



[View related articles](#)



[View Crossmark data](#)



## Geology of the lower Belice River valley, epicentral area of the $M > 5$ 1968 seismic sequence (south-western Sicily, Italy)

Stefano Pucci <sup>a</sup>, Giuseppe Avellone <sup>b</sup>, Antonio Contino <sup>b</sup>, Alessandro Incarbona <sup>b</sup>, Leonardo Sagnotti <sup>a</sup>, Attilio Sulli <sup>b</sup>, Enrico Di Stefano <sup>b</sup>, Alessandra Smedile <sup>a</sup>, Anna Maria Gueli<sup>c</sup> and Giuseppe Stella<sup>c</sup>

<sup>a</sup>Istituto Nazionale di Geofisica e Vulcanologia, Roma, Italy; <sup>b</sup>Dipartimento di Scienze della Terra e del Mare, Università degli Studi di Palermo, Palermo, Italy; <sup>c</sup>Dipartimento di Fisica e Astronomia, Università degli Studi di Catania, Catania, Italy

### ABSTRACT

We present a new 1:25,000-scale geological map of the lower Belice River valley, the area struck by the  $M > 5.0$  devastating 1968 seismic sequence, whose seismic source and seismotectonic framework are still controversial. The map, utilizing dating methods and traditional field survey approaches integrated by high-resolution topography, provides an unprecedented detail and precision on the spatial distribution and on the compressional growth geometries of the prominent sedimentary sequence. This map, supported by the first recognition of an on-shore Chibanian-Calabrian deposition and by identifying a flight of marine terraces, offers new insights on the long-lasting syn-depositional tectonic forces up to late-Pleistocene-Holocene times. Such tectonic forces may take part in the regional ongoing deformational phase, prompting detailed studies on the potential seismic sources affecting the area.

### ARTICLE HISTORY

Received 9 February 2023  
Revised 12 July 2023  
Accepted 25 July 2023

### KEYWORDS

Geology; quaternary deposit; biostratigraphy; active tectonics; earthquake; LiDAR

## 1. Introduction

The study area is located in the southwestern part of Sicily, along the lower valley of the south-flowing Belice River (Figure 1). Here, the river crosscuts the periclinal termination of the WNW-ESE-trending and SSW-verging Mt. Magaggiaro anticline, the south-westernmost on-shore compressional structure of the Sicilian fold-and-thrust belt, which is a sector of the Apenninic-Maghrebian orogen (Bello et al., 2000; Catalano et al., 2000, 2013; Goes et al., 2004; Gueguen et al., 1998). The Mt. Magaggiaro anticline is set over the western tip of the arc shaped, N-dipping main thrust system, the Gela Basal Thrust (hereinafter GBT), ahead of the sharp attitude change of the NE-SW-striking thrust system of the westernmost Sicily.

The Belice River incises and exposes a complete depositional sequence, from the Meso-Cenozoic fold core to the Pliocene-Pleistocene deposits of two large wedge-top basins, the Belice and the Menfi basins; the first, north of the anticline, is filled by the 50-400 m thick Plio-Pleistocene Marnoso Arenacea del Belice Formation (Fm.), characterized by growth geometries and sedimentary structures that highlight the activity of the bounding anticlines (Di Stefano & Vitale, 1993; Vitale, 1995); the second, in the forefront of the anticline, is formed by 50-900 m thick, Plio-

Pleistocene bioclastic and clayish deposits that dip toward the shoreline and are intercepted and imaged onshore by Agip Menfi1 and Marinella 2 wells (Videpi project, [www.videpi.com](http://www.videpi.com)) and seismic section (respectively Main Map and Figure 1).

Data from seismic lines and well logs show that the Mt. Magaggiaro anticline represents the culmination of a much larger (i.e. long-wavelength) ramp anticline. This is characterized by a main high-angle thrust, flattening at a depth of about 2.5 km and buried at 1–2 km, doubling the top of Saccense succession (see blue and green line, Figure 1(b)). Since the originally flat thrust plane was folded and displaced by a later high-angle thrust ('deep seated thrust' sensu Avellone et al., 2010), a multiphase tectonic deformation can be invoked.

We point out that in the adjoining sector, W of the Belice River, both the exposed and buried structures (occurring also in the offshore area of western Sicily) have perpendicular NE-SW trends (Figure 1(a)). Some of them are assumed to have been active starting from 0.8 to 1.2 Ma (e.g. Castelvetro thrust, Barreca et al., 2014). This abrupt change of the structural trend is also visible at regional scale ('double-arch' shape of Sicily chain front; Figure 1(a)). Conversely, E of the Belice River the tectonic setting is more regular: the

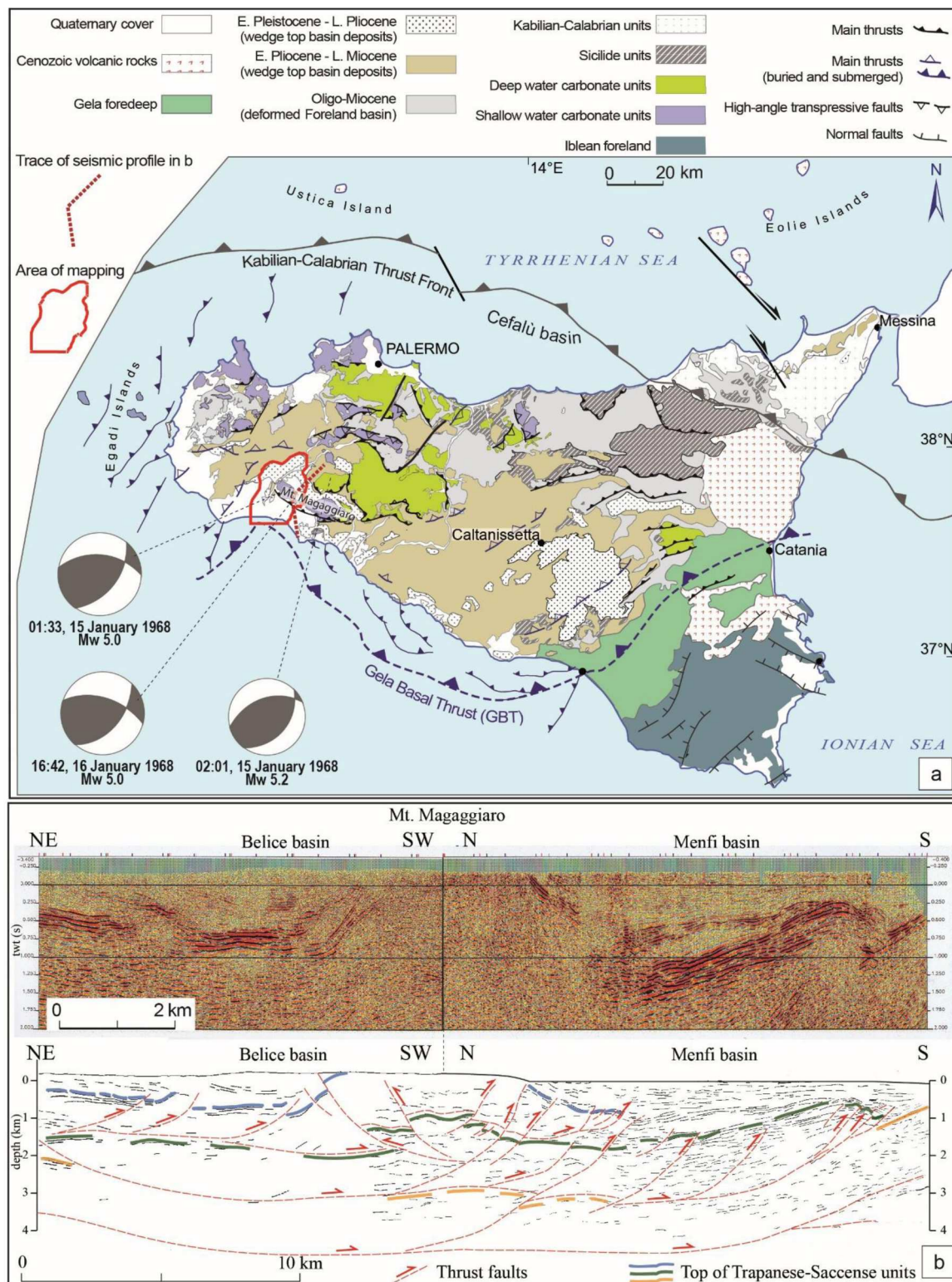


**Figure 1.** (a) Sketch of the main tectonic structures of Sicily (modified from Catalano et al., 2013). The focal solutions of the 1968 seismic sequence mainshocks are reported (Orecchio et al., 2021); (b) Time-migrated seismic reflection line image showing the main markers (the traces amplitude is represented as variable density area with a red-yellow-white-black color palette – black: positive polarity; red: negative polarity) and its interpretative line drawing with the tectonic structures of the study area (from Catalano et al., 2000). Deep AGIP wells (<https://www.videpi.com>) used as constraints are located in the main map.

trace of the axial surface of the Magaggiaro anticline rotates gradually (by as little as  $30^\circ$ , from NW-SE in the Mt. Magaggiaro-Mt. Arancio sector to E-W in the Pizzo Telegrafo one), resulting in a slightly arcuate shape in the map (Figure 1). The regional structure is

made up of three imbricated Meso-Cenozoic shallow water carbonate thrust sheets (Saccense tectonic units), showing a southwestern vergence, as part of the southwest-Sicily compressional seismotectonic province (Lavecchia et al., 2007).

Southwestern Sicily presents a moderate-to-low seismic hazard with a local maximum extending along the Belice Valley (Peak Ground Acceleration of up to 0.1 g at 10% of probability in 50 years; Meletti et al., 2021). Here, since the historical earthquakes that caused the collapse of the Greek temples at the Selinunte archaeological site in historical times (3th-4th century BCE and 6th-thirteenth century CE; Guidoboni et al., 2002), the following events of the 18-twentieth century CE did not exceed magnitude 5 (Rovida et al., 2020). On 14–25 January 1968, the Belice seismic sequence occurred with six main shocks producing the highest values of macroseismic intensity of X ( $I_{MCS}$ ), corresponding to events of 5.1–6.4 in magnitude ( $M_w$ ) (Guidoboni et al., 2019; Rovida et al., 2020, Figure 1(a)). It led to 231 official victims (possibly underestimated), thousands of injured people and about 100,000 homeless. The complete collapse of 90% of the rural edifices (~3000) in the epicentre area, requiring delocalized post-earthquake reconstruction of villages, triggered a significant economic crisis that provoked a relevant human migration (Barbera, 1980).

The 1968 seismic sequence represents the largest instrumental event of the Sicily Island, testifying the tectonic activity of this region. However, there is still poor knowledge on location, geometric and kinematic parameters of the main seismogenic structures (DISS Working Group, 2018). Seismological data of the best-constrained events show hypocentres between 13 and 36 km in depth and uncertain focal mechanism solutions. E-W and/or ~N-S-trending nodal planes suggest kinematics ranging from pure thrust to strike-slip (Anderson & Jackson, 1987; Gasparini et al., 1985; McKenzie, 1972; Orecchio et al., 2021). These are compatible with either the N-dipping GBT (see Lavecchia et al., 2007; Monaco et al., 1996) or with the N–S-trending right-lateral lithospheric strike-slip fault system responsible for the differential flexural retreat of the Pelagian foreland, respectively (Cardamone et al., 1976; Finetti & Del Ben, 2005; Gasparini et al., 1985; Meletti et al., 2000; Michetti et al., 1995) (Figure 1(a)). In the context of the Late Quaternary coastal uplift of southwestern Sicily (up to ~0.75 mm/a; Ferranti et al., 2021), contrasting geological evidence of active structures in the Belice area have previously been reported in maps and scientific papers: despite the blind steep north-dipping reverse faults, inner splays of the GBT, and active strike slip lineaments (Barreca et al., 2014; Michetti et al., 1995; Monaco et al., 1996; Tondi et al., 2006), Quaternary N-dipping normal faults were reported (Di Stefano & Vitale, 1993).

Here we show a geological-geomorphological map built through a multidisciplinary study, integrating intensive field survey, aerial-photo interpretation and high-resolution LiDAR analysis with seismo-

stratigraphic, micropaleontological and paleomagnetic data. The study provides a modern cartographic tool for territorial planning of a large area of Sicily that is lacking updated geological cartography. In fact, this area is partially covered by the recent 1:50,000-scale Italian Geological Map (Sheet 619 ‘Santa Margherita Belice’, 2013), with the most part charted by old 1:100,000-scale Italian Geological Map (Sheet 265 ‘Mazzara del Vallo’, 1955; Sheets 257 ‘Castelvetrano’, 258 ‘Corleone’, 266 ‘Sciacca’, 1882, see ISPRA <https://www.isprambiente.gov.it/it/attivita/suolo-e-territorio/cartografia/carte-geologiche-e-geotematiche>). The mapping focused on sharpening the Quaternary continental and marine deposits sequence and detailing the surface expression of the tectonic structures. As a result, this geological map (Main Map) provides an improved support for the reconstruction of the recent tectonic evolution of the study area and represents the necessary background for further studies on the characterization of its active tectonics.

## 2. Methodology

We present a map of the lower Belice River Valley (Main Map) surveyed at 1:10,000-scale and published at 1:25,000-scale, covering an area of about 330 km<sup>2</sup>. The mapping is mainly based on field reconnaissance and collection of new geological data that critically integrates, and in some cases deeply revises, the previously published maps (Di Stefano et al., 2013; Di Stefano & Vitale, 1993), with particular focus in detailing the Quaternary depositional facies of both continental and widespread marine deposits. For the survey, we adopted the regional topographic basemap (Carta Tecnica Regionale 1:10,000). Moreover, the main map strongly benefited from the interpretation of 1:33,000 scale aerial photographs (Istituto Geografico Militare, 1954/1955), 25 cm/pixel orthophoto raster imageries (flight ATA 2012-2013, Regione Siciliana, [www.sitr.regione.sicilia.it/geoportale/it](http://www.sitr.regione.sicilia.it/geoportale/it)) and from a 2 m/pixel DTM derived from airborne LiDAR (Light Detection And Ranging; flight ATA 2007-2008, Regione Siciliana – [www.sitr.regione.sicilia.it/geoportale/it](http://www.sitr.regione.sicilia.it/geoportale/it)), as well as from its derivative digital maps (shaded relief, slope, aspect, drainage network, etc.). In fact, they yielded the possibility to detect subtle geomorphic signatures related to tectonics and lithology in areas of dense vegetation (e.g. Arrowsmith & Zielke, 2009) and allowed us to refine and trace geological contacts (i.e. the morpho-stratigraphical separation of different units), bedding attitudes, fault traces and geomorphic features (e.g. fault scarps).

The deep structural setting is interpreted in the provided cross section (A-A’ in Main Map) by integrating information from a grid of multichannel commercial seismic reflection profiles (AGIP zone AG year 1980;

see Catalano et al., 2000) crossing the Belice and Menfi basins, and calibrated by Agip well logs (Melfi\_001 and Marinella\_002 wells) (<https://www.videpi.com>; see Catalano et al., 1998) (Figure 1(b)). Seismic units were identified based on seismic attributes and geometries and interpreted in terms of sequence stratigraphy.

## 2.1. Pre-quaternary stratigraphy

The pre-Quaternary substrate is represented by: Upper Triassic-Early Jurassic carbonate platform succession evolving to Middle-Late Jurassic condensed ammonitic deposits; Late Jurassic-Eocene pelagic carbonate and Oligocene-Miocene marly-clayey terrigenous covers. These deposits pertain to the Saccense domain (see stratigraphic column in the Main Map). We mapped the stratigraphic sequence of the pre-Quaternary substrate following the subdivision already proposed by Basilone (2012 and reference therein). Considering the focus on the Quaternary period, we reported this sequence without internal subdivision, incorporating some of them within a single informal unit.

From the bottom, this succession consists of:

### 2.1.1. Sciacca, Inici and Buccheri Fms. (TGL) (Late Triassic-Late Jurassic)

White limestones and dolomitic limestones with algae and mollusks, of back-reef lagoon, tidal flat and sand barrier environments, with peritidal cycles. Upwards it presents oolitic-bioclastic calcarenites and evolves to condensed and pelagic nodular ammonitic limestones with interbedded breccias. The minimum outcropping thickness is up to 300 metres, but it can reach more than 3000 metres according to seismic profiles and exploration wells.

### 2.1.2. Lattimusa and Hybla Fms. (MLC) (Late Jurassic-Early Cretaceous)

Greenish marls and white cherty marly calcilutites of a pelagic carbonate platform to open shelf marine environment with benthic and planktonic foraminifera, radiolarians and calcareous nannofossils. About 40 metres thick.

### 2.1.3. Amerillo Fm. (LCP) (Late Cretaceous-Eocene)

White calcilutites with nodules of chert, alternate marly calcilutites and marls with planktonic foraminifera and layers of calcareous megabreccias with clasts of carbonate platform. It is followed by bioturbated marly limestones with nummulitic calcarenites and green sandy, clayey marls and sands, with planktonic foraminifera (80-150 m thick).

### 2.1.4. Marne di Cardellia, Ragusa, Calcareniti di Corleone, Marne di San Cipirello and Terravecchia Fms. (SCM) (Oligocene-Early Messinian)

White-yellow-greenish calcarenites and marly carbonates with Lepidocyclinae, Miogypsinae, crinoids and *Nummulites* spp. (Marne di Cardellia and Ragusa Fms.). Biocalcirudites, biocalcarenes and glauconitic sandstones of open shelf environment with cross-stratification and alternate with brown-greenish sandy marls (Calcareniti di Corleone Fm.), covered by clays, sandy clays and brown marls with planktonic foraminifera (Marne di San Cipirello Fm.). On the top are present terrigenous deposits consisting in grey-greenish clays and sandy marls with intercalations and lenses of conglomerates with sandy matrix (Terravecchia Fm.). Overall 200–400 metres thick.

### 2.1.5. Gessoso-Solfifera Group (EVM) (Messinian)

Clastic and selenitic gypsum and gypsarenites, 30–50 metres thick.

### 2.1.6. Trubi Fm. (MLP) (Zanclean-Early Piacenzian)

Marls and marly limestones with calcareous plankton of bathyal environment and local megabreccias of Triassic-Jurassic carbonate clasts, 30–50 metres thick (Figure 2(a)).

### 2.1.7. Marnoso-Arenacea del Belice Fm. (BAG, TCG) (Piacenzian-Gelasian)

Shallow water white-yellowish cross-stratified calcarenites (BAG) with benthic foraminifera (*Amphistegina* spp.), algae, bryozoans, mollusks and corals, frequently highly bioturbated, 50-400 m thick. BAG is laterally heteropic with outer shelf turbiditic grey-blue marly clays (TCG) (Figure 2(a)).

## 2.2. Quaternary stratigraphy

The reconstructed stratigraphic sequence is the result of the refinement of the one suggested by Di Stefano et al. (1991) with the introduction of new Middle Pleistocene (Chibanian Stage) and Late Pleistocene-Holocene marine units.

Apart from the recognition of distinct sedimentary facies and facies associations, new microfaunal content (Table 1) and paleomagnetic data (Table 2) were analysed in order to discriminate the chronostratigraphic framework and to allow a more reliable correlation between Quaternary sedimentary bodies. The microfaunal content also supported the differentiation of marine deposits from continental units and, for the latter, we used lithostratigraphy as the main criterion of distinction.

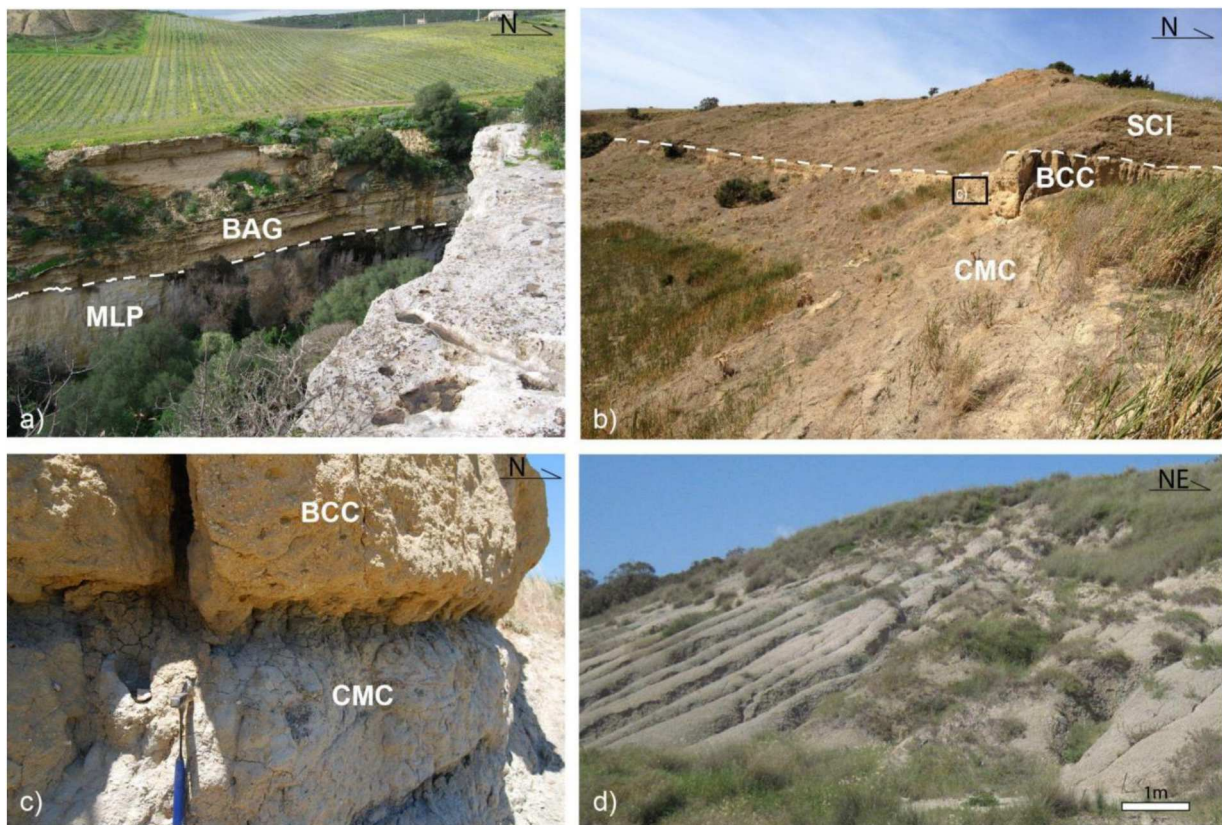


**Figure 2.** (a) Top of the whitish marly limestones of the Trubi Fm. (MLP) and paraconformity with the bottom of the yellowish calcarenites of the Marnoso-Arenacea del Belice Fm. (BAG). (b) View of the 1-m-thick bioclastic Calabrian calcarenite (BCC) at the top of the blue-grey Calabrian clayey marls (CMC). (c) Detail of the 1-m-thick bioclastic Calabrian calcarenite (BCC) showing loading pockets, bioturbations and macrofauna. (d) Grey-brownish Calabrian-Chibanian clay (SCI) outcrop sampled for both paleomagnetic and biostratigraphic analyses. Locations: Contrada Riserva, Case Catarinicchia and Porto Palo in Main Map, respectively.

### 2.3. Microfaunal content analysis

Calcareous nannofossil assemblages were investigated on 35 samples (Figure 3 and Table 1). The analysis was carried out by observation with a polarized microscope at about 1000× magnification, in rippled smear slides prepared following the standard procedure (Bown & Young, 1998). Axiocam Cci camera and software Axiovision 4.7 were used for length measurements of coccoliths. The instrumental uncertainty due to the Axiovision 4.7 software is of 0.005 μm (1 pixel) and is therefore negligible. A further error in measurements may be given by the tilt of coccoliths. However, the error would become significant (>5%) for angles  $\geq 20^\circ$ , a tilt that is rather unlikely and would prevent the correct identification of taxa (Di Stefano et al., 2014). The regional Pliocene/Pleistocene biostratigraphic scheme and taxonomic concepts of Rio et al. (1990) were adopted. Specifically, the biometric subdivision of the genus *Gephyrocapsa* follows Rio (1982) and Rio et al. (1990): small *Gephyrocapsa* includes specimens <4 μm, medium *Gephyrocapsa* includes specimens between 4 and 5.5 μm, large *Gephyrocapsa* includes specimens >5.5 μm. Specimens of *Gephyrocapsa omega* (*Gephyrocapsa* sp.3 sensu Rio, 1982) includes

specimens >4 μm with a high bridge angle (the bridge is almost aligned to the short axis of the placolith).

### 2.4. Paleomagnetic analysis

A total of 25 discrete samples of fine-grained sediments (mostly marine silty and sandy clays), available in 5 outcrops, were taken using oriented standard plastic boxes (8 cm<sup>3</sup>) to examine their paleomagnetic properties and polarity (see Main Map for location). In order to avoid the deformation of the sediment, the deposit free face was pre-cut using a thin stainless steel spatula before pressing the plastic boxes into the outcrop.

All the samples were analysed at the paleomagnetic laboratory of the Istituto Nazionale di Geofisica e Vulcanologia, in Rome, on a small access (45 mm diameter) automated pass through '2G Enterprises' DC 755 superconducting rock magnetometer, installed in a magnetically shielded room and equipped with a standard air-cooled solenoid and a transverse split pair, for in-line orthogonal alternating field (AF) demagnetization. To investigate the stability of the natural remanent magnetization (NRM) of the samples and to reveal possible secondary overprints,

**Table 1.** List of significant samples examined for nannofossil biostratigraphic analysis.

Sample ID	Lithology (map code)	Location: Name; Lon; Lat (CGS WGS84); Elev (m a.s.l.)	Stage	Biozones
8	SCI	Contrada Marzucchi; 12.8715; 37.6413; 110	Calabrian-Chibanian	(MNN 19f) <i>Gephyrocapsa omega</i> , <i>P. lacunosa</i>
9	CMC	Contrada Case Nuove; 12.8991; 37.6315; 110	Calabrian	(MNN 19e) <i>small Gephyrocapsa</i>
20	CMC	Piana di Cavotta; 12.8996; 37.6569; 30	Calabrian	(MNN 19B-C) <i>medium Gephyrocapsa</i>
59	SCI	Contrada Marzucchi; 12.8717; 37.6428; 110	Calabrian-Chibanian?	(MNN 19f) <i>Gephyrocapsa omega</i> , <i>P. lacunosa</i>
60	SCI	Contrada Serrone Cipollazzo; 12.9217; 37.5773; 10	Pleistocene	<i>Gephyrocapsids</i> , <i>P. lacunosa</i>
61	SCI	Contrada Serrone Cipollazzo; 12.9221; 37.5775; 15	Pleistocene	<i>Gephyrocapsids</i> , <i>P. lacunosa</i>
62	SCI	Contrada Serrone Cipollazzo; 12.9223; 37.5776; 20	Pleistocene	<i>Gephyrocapsids</i> , <i>P. lacunosa</i>
67	SCI	Miramare; 12.9104; 37.5779; 10	Pleistocene	<i>Gephyrocapsids</i> , <i>P. lacunosa</i>
71	SCI	Villaggio Catalano; 12.8532; 37.5916; 45	Chibanian	(MNN 19f) <i>Gephyrocapsa omega</i> , <i>Gephyrocapsa caribbeana</i>
81	SCI	Miramare; 12.9101; 37.5780; 10	Chibanian	(MNN 19f) <i>Gephyrocapsa omega</i> , <i>Gephyrocapsa caribbeana</i>
82	SCI	Miramare; 12.9101; 37.5781; 14	Chibanian	(MNN 19f) <i>Gephyrocapsa omega</i> , <i>Gephyrocapsa caribbeana</i>
83	SCI	Miramare; 12.9101; 37.5782; 17	Chibanian	(MNN 19f) <i>Gephyrocapsa omega</i> , <i>Gephyrocapsa caribbeana</i>
84	SCI	Miramare; 12.9101; 37.5784; 20	Chibanian	(MNN 19f) <i>Gephyrocapsa omega</i> , <i>Gephyrocapsa caribbeana</i>
85	SCI	Miramare; 12.9100; 37.5785; 23	Chibanian	(MNN 19f) <i>Gephyrocapsa omega</i> , <i>Gephyrocapsa caribbeana</i>

In biozones, the name of distinctive taxa is reported. See Main Map for locations.

all samples were stepwise AF demagnetized in peak fields of 5–10–15–20–30–40–50–60–80–100 mT, with remanence vectors measured after each demagnetization step.

17 samples from 4 sites gave interpretable demagnetization diagrams and showed an almost single-component NRM: after the removal of a low-coercivity component at 5–10 mT, the paleomagnetic direction remains stable up to 40–50 mT, with demagnetization vectors aligned along linear paths towards the origin in orthogonal vector diagrams. Therefore, a clear and well-defined characteristic remanent magnetization (ChRM) has been isolated for each of these samples and its direction computed by principal component analysis on at least four consecutive steps at AF peak values between 15 and 50 mT, using the DAIE software (Sagnotti, 2013). The paleomagnetic results are listed in Table 2. The overall paleomagnetic mean, computed by Fisher statistics (Fisher, 1953) indicates a mean paleomagnetic declination and inclination of 354.6° and 42.3°, respectively, with a half-angle of the cone of 95% confidence about the mean direction of 9.1°, which – apart from a sedimentary inclination flattening – is close to the expected direction for a geocentric axial dipole field in this region (decl = 0°; incl = 56°) and indicates a normal paleomagnetic polarity for all samples.

## 2.4. Marine units

### 2.4.1. Calabrian clayey marls (CMC) and calcarenites (BCC)

Blue-grey clayey marls (CMC) alternating with (and laterally passing to) bioclastic calcarenites with *Arctica*

*islandica* (BCC), testifying to a circalittoral and epibathyal environment (D'Arpa & Incarbona, 2022; Di Stefano et al., 1991), with occurrence of high-energy tractive currents having lateral transition to the low energy platform environment (Figure 2(b,c)). At its top this unit presents 1-m thick biocalcarenic bank (BCC) referred to as MIS 22 (D'Arpa & Incarbona, 2022; Di Stefano et al., 1991) and characterized by load casts along the basal sand-mud interface (Figure 2(c)).

CMC is made by blue to grey clayey marls (near 22% of carbonate, Di Stefano et al., 1991), is locally bioturbated and gradually coarsens upward to calcisiltite and fine-grained yellowish sandstones (Di Stefano et al., 1991). It presents macrofauna, such as bivalves and gastropods (*Venus* spp., *Turritella* spp., *Aporrhais* spp.), serpulids (*Ditrupa arietina*), echinoids fragments, and microfossil assemblage characterized by ostracods (*Henryhowella sarsii*, *Bairdia conformis*), planktonic and benthic foraminifera (*Globorotalia truncatulinoides excelsa*, *Hyalinea baltica*) and calcareous nannofossils (*Gephyrocapsa omega*, *Pseudoemiliana lacunosa*).

BCC is composed of normally graded bioclastic light yellow calcarenites and rare conglomerates with internal unconformities and prograding clinofolds. It contains abundant foraminifera, echinoids, sponges, bryozoans, scaphopods, vermetids, gastropods (*Patella* spp.), bivalves (*Turritella communis*, *Glycymeris* spp., *Pecten jacobaeus*, *Talochlamys multistriata*, *Pseudamussium peslutrae*, *Arctica islandica*, *Ostrea* spp.), ostracods (*Bythocythere turgida*), pteropods (*Limacina retroversa*) and fragments of red calcareous algae (*Lithothamnium* spp.).

**Table 2.** Samples data of paleomagnetic analysis (Miramare; Figure 2(d)); DIM: Contrada Dimina; MAR: Marinella (see Main Map for location).

Sample ID	Lithology (map code)	Location: Name; Lon.; Lat. (CGS WGS84); Elev. (m a.s.l.)	AF steps (mT)	Decl ChRM (°)	Incl ChRM (°)	MAD (°)
PP01	SCI	Contrada Serrone Cipollazzo; 12.9196; 37.5778; 12	15–40	8.0	27.2	5.6
PP02	SCI	Contrada Serrone Cipollazzo; 12.9197; 37.5779; 21	15–40	322.7	45.3	9.5
PP03	SCI	Contrada Serrone Cipollazzo; 12.9197; 37.5780; 27	15–40	342.5	51.9	1.6
PP04	SCI	Contrada Serrone Cipollazzo; 12.9197; 37.5781; 33	15–40	2.8	46.1	0.9
P1	SCI	Miramare; 12.9100; 37.5780; 8	15–50	338.5	50.7	1.4
P2	SCI	Miramare; 12.9100; 37.5782; 20	15–50	339.1	44.2	1.8
P3	SCI	Miramare; 12.9099; 37.5785; 29	15–40	330.4	44.2	3.4
DIM2	SCI	Contrada Dimina; 12.8561; 37.6403; 108	15–40	330.5	47.0	4.3
DIM3	SCI	Contrada Dimina; 12.8561; 37.6403; 108	15–40	358.1	50.5	5.1
DIM6	SCI	Contrada Dimina; 12.8776; 37.6357; 113	15–40	20.9	38.8	4.2
DIM7	SCI	Contrada Dimina; 12.8776; 37.6357; 113	15–40	5.1	75.2	5.2
DIM8	SCI	Contrada Dimina; 12.8776; 37.6357; 114	15–40	11.9	29.7	4.8
MAR01	SCI	Marinella; 12.8412; 37.5820; 10	20–40	4.0	17.5	2.4
MAR02	SCI	Marinella; 12.8408; 37.5821; 9	20–40	25.5	28.0	4.6
MAR03	SCI	Marinella; 12.8405; 37.5823; 14	20–40	347.7	22.1	14.6
Fisher statistics						
			<b>N of samples</b>	<b>Decl ChRM (°)</b>	<b>Incl ChRM (°)</b>	<b><math>\alpha_{95}</math> (°)</b>
Mean			17	354.6	42.3	9.1

AF steps: alternating field (AF) demagnetization steps used to compute the Characteristic Remanent Magnetization (ChRM) with principal component analysis, using the DAIE software (Sagnotti, 2013); Decl: Declination of the ChRM; Incl: Inclination of the ChRM; MAD(°): Maximum Angular Deviation;  $\alpha_{95}$  (°): half-angle of cone of 95% confidence about the mean paleomagnetic direction computed with Fisher statistics (Fisher, 1953).

This formation presents a reduced thickness of 70 m, near to Mt. Magaggiaro Anticline, where it unconformably covers, with the dominant calcarenitic lithofacies (BCC), the pre-Quaternary substratum and forms the Montevago-S.M. Belice paleosurface. South of the Mt. Magaggiaro Anticline, the prevailing clayey lithofacies (CMC) paraconformably overlaps the

Pliocene deposits (Figure 2(a)), as documented by the onshore Menfi well (Catalano et al., 1998), where it thickens to 600-900 m.

These two lithotypes are equivalent to those of the Agrigento Fm. and of Marsala Synthem (Di Maggio et al., 2009 and references therein) and are ascribed to part of the Calabrian Stage, Emilian and Sicilian

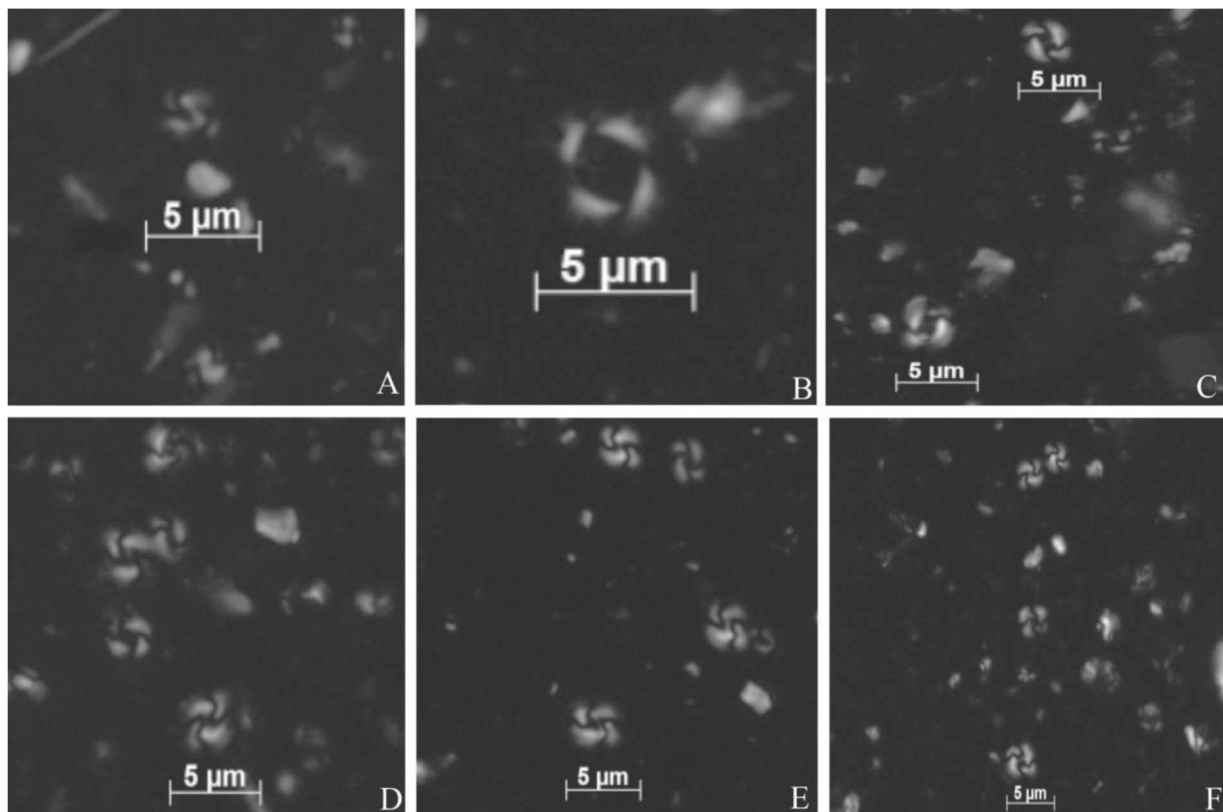


**Figure 3.** Selected calcareous nannofossils in Belice Valley samples. Snapshots of polarized light microscope, X nicols. Size bars are included. (A): small *Gephyrocapsa acme* in sample 10\_09. (B): *Pseudoemiliana lacunosa* in sample P1. (C): *Gephyrocapsa omega* in sample 10\_08. (D): *Gephyrocapsa caribbeanica acme* in sample P3. (E): *Gephyrocapsa caribbeanica acme* in sample P4. (F): *Gephyrocapsa caribbeanica acme* in sample P4.



Substages *sensu* Ruggieri et al. (1984), Ruggieri and Unti (1974), Ruggieri and Sprovieri (1983), Di Stefano et al. (1991) and Di Geronimo et al. (1994).

#### 2.4.2. Calabrian – Chibanian clay (SCI, BCI)

Gray-brown clay (SCI) alternating with sandy calcarenites and lenses of well-cemented bioclastic calcarenites (BCI) (Figure 2(d)), of circalittoral and epibathyal environments, respectively (Di Stefano et al., 1991; D'Arpa & Incarbona, 2022). This unit contains abundant foraminifera and calcareous nannofossils, respectively belonging to *Globorotalia truncatulinoides excelsa* and *Pseudoemiliania lacunosa*

biozones (Di Stefano et al., 1991). It passes upwards to channelized sandy clay and fine sands with abundant bioclastic debris and with serpulids (*Ditrupa arietina*) and mollusks (*Turritella communis* and pectinids).

#### 2.4.3. Marine Terrace deposits (SCP) (Middle-Late Pleistocene)

Thin foreshore deposits with planar- and/or cross-laminated lithoarenites (Figure 4(a–c)), planar cross-bedded sandstones and transgressive basal conglomerate with quartz-arenitic pebbles locally showing marine potholes (Figure 4(d)). These deposits consist of yellowish to reddish, well-sorted quartz-derived



**Figure 4.** Marine terraces and continental deposits. (a) Foreshore cross-bedded lithoarenites. (b, c) Thin foreshore lithoarenites (SCP) unconformably lying on fersiallitic, bioturbated paleosols at the top of the Calabrian and Chibanian circalittoral/epibathyal marine deposits (BCI). (d) Marine potholes carved in the foreshore lithoarenites. (e, f) Loose gravels and pebbles of well-rounded and flattened quartz-arenite of reworked Numidian flysch. Locations: Porto Palo, Contrada Dimina and Contrada Latomie in Main Map, respectively.

sand, weak- to well cemented, with abundant layered quartzitic gravels and subordinate well-rounded quartz-arenitic pebbles. They are sterile in both micro- and macrofauna. They unconformably overlie erosional surfaces carved on the Calabrian and Chibanian circalittoral/epibathyal marine deposits (Figure 4 (b,c)), characterized by fersiallitic, bioturbated paleosoils developed over yellowish marine sands with small fragments of bryozoans and mollusks (up to 4 m thick) and contain rare decimeter-thick lenses of grey-blue marls.

## 2.5. Continental deposits

### 2.5.1. Quartz-arenite pebbles and gravels (RDP) (Calabrian?-Holocene)

This unit consists of abundant loose, quartz-arenite pebbles in brown-blackish silty and occasionally clayey sand matrix and includes gravels, weakly cemented, with well-rounded and flattened quartz-arenite pebbles. They frequently cover the shoreface quartzitic sand of the Marine Terrace deposits and locally the early Calabrian calcarenites. The mature, flattened pebbles are possibly derived from the fluvial reworking of the Numidian flysch, which outcrops upstream of the local drainage systems (Figure 4(e,f)).

### 2.5.2. Aeolian sand (SDI, SDH) (Late Pleistocene-Holocene)

Reddish to whitish quartzitic sands with metric cross-lamination, at places separated by dark grey paleosoils. The medium to coarse and well-sorted quartz grains, from loose to poorly cemented, form dunes fields at the back of paleo- (SDI) and present-day (SDH) shorelines. For the archaeological site of Selinunte, [Ortolani and Pagliuca \(1995\)](#) ascribed these deposits (loose or poorly cemented) to the Holocene.

### 2.5.3. Alluvial (ALP, APH, AFH, ALH) and fluvial (FLH) deposits (Late Pleistocene-Holocene)

Flat conglomerates, gravels and sands, in a silty matrix, locally with layered tractive structures, barren in micro and macrofauna, overlain by a pedogenized silty-clayey sheet. Alluvial fans (AFH, APH) are organized in polycycles of heterogenic conglomerates and sands. Flooding deposits (ALH, ALP) are mainly composed of gravels and sand with an abundant silty matrix. Thalweg deposits (FLH) present cross-stratification and structures of channelized fluxes. The deposits that are no more in relation with the present-day fluvial dynamics (ALP, APH) are organized in a flight of inset cut terraces, up to 5 m thick, that unconformably rest over erosional surfaces carved in both pre-Quaternary and Quaternary marine substrata.

### 2.5.4. Eluvial (EPH) and colluvial (COH) deposits and Paleosoils (Late Pleistocene-Holocene)

Reddish to yellowish-brown pelitic and/or sandy matrix with heterogeneous, heterometric and immature clasts, locally more than 3 m thick, as result of pedogenic processes and/or mobilization of deposits by runoff processes ([Wagner et al., 2007](#)). The pedogenic thickness increases with elevation, with maximum thickness of reddish and kaolinitic sand at the top of the Mt. Magaggiaro and Montevago-S.M. Belice paleosurface.

### 2.5.5. Beach deposits (SBH) (Holocene)

Loose deposits of low-sorted, mature, fine to medium quartzitic sand with ripples at the present-day shoreline.

## 2.6. Structural features

The NW-SE trending Magaggiaro anticline exhibits a periclinal termination due to a NW dip of the fold axes and multiple thrusts on both limbs, depicting a double-vergence pop-up structure (see cross-section in Main Map). Along the southern limb, the folded Miocene succession shows a steep attitude documenting the southwestern vergence. Along its northern limb, a SW-dipping, NW-SE-striking high-angle back-thrust juxtaposes Triassic-Jurassic limestones to Plio-Pleistocene clays and calcarenites, with the involvement of some secondary splays and outcropping mesoscopic fault planes (Figure 5).

The Belice and Menfi basins developed as Plio-Pleistocene thrust-top basins (according to [Vitale & Sulli, 1997](#); [Catalano et al., 1998, 2000](#), Figure 1(a)). The Belice basin is filled up by about 1000 m-thick deposits, showing clinoform packages truncated by plane-parallel sequences: the upper S. Margherita-Montevago terrace (350-390 m a.s.l.), testifying a shoreline regression leaving space to the continental environment. The Menfi basin fills a flexural basin where the Pliocene-Chibanian marine units present a clinoform profile depicting basinward divergent stratigraphic boundaries (i.e.: grow-strata) and down-step stratigraphic terminations (i.e.: off-lap, see geological section in Main Map). The latter is transgressively overlain by a flight of marine terraces, up to about 400 metres a.s.l., covered by paleosoils and continental conglomerates of regressive sequences.

## 3. Conclusions

A new geological map of the lower Belice River valley is provided with the distinction of internal stratigraphy of the marine Pleistocene sequence. The mapping was conducted to grasp the spatial distribution and the paleoenvironmental significance of the deposition (and its evolution) potentially associated with tectonic

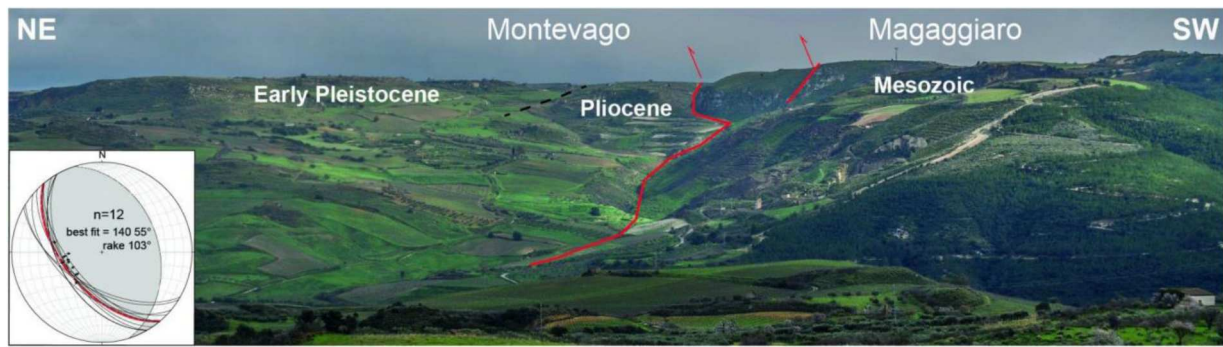


**Figure 5.** Panoramic view of the Magaggiaro paleosurface (SE-looking). The paleosurface was recognized to be dissected by a high-angle back-thrust. The inset shows the best fit fault plane and kinematics from faults measured in the field (plotted by Fault-Kin 8.1, Richard W. Allmendinger ©). No extensional faulting is responsible for the tectonic juxtaposition of Plio-Pleistocene and Mesozoic formations.

forcing. In addition, we point out the reconstruction of outcropping fault systems and the identification of their kinematics.

### 3.1. Stratigraphy

Both biostratigraphic and paleomagnetic analysis were conducted for the chronostratigraphic assignment of the lithofacies, with particular focus on the distinction of the on-shore Calabrian-Chibanian deposits. 21 samples were useful for their content in nannofossils: most of them can be ascribed to the MNN 19f Zone (occurrence of specimens of *Gephyrocapsa omega* and *P. lacunosa*), a biozone that covers the 1.0-0.5 Ma interval and thus helped the first recognition of an on-shore Chibanian-Calabrian deposition; five samples collected in the Porto Palo section may be ascribed to the middle/upper part of the MNN 19f Zone. They show taxonomic sequences where specimens of *Gephyrocapsa omega* at the base of the sedimentary sequence become rather rare upwards, leaving space for abundant *Gephyrocapsa caribbeanica*. This resembles the dominance intervals in the evolutionary lineage of the late Quaternary (e.g. Baumann & Freitag, 2004; Flores et al., 2000, 2003; Hine & Weaver, 1998; Villanueva et al., 2002) and recognized even in the central Mediterranean Sea down to 0.4 Ma (Incarbona et al., 2009). All the samples that gave reliable paleomagnetic data revealed a normal magnetic polarity, compatible with a deposition during the Brunhes Chron. In general, the biostratigraphic and paleomagnetic data collected from the top of the pelagic sequence that outcrops near the present-day shoreline suggest a Chibanian age.

### 3.2. Structural setting

The geological map reveals tectonic features that are mainly associated with the NW-SE trending Mt. Magaggiaro anticline activity (Main Map). Truncated clinoform packages at the backlimb of the Magaggiaro anticline, grow-strata and off-lap at its forelimb, as

well as the presence of flights of marine and fluvial terrace deposits, testifies the occurrence of tectonically-forced shoreline migration of a marine regression. Progressive tectonic growth is demonstrated by integrated well data and field data collected along the southern buried limb of the anticline. Overall, collected data suggest the growth of the anticline occurred during the Calabrian-Chibanian time interval (see geological cross-section on the main map).

Moreover, the high-angle Mt. Magaggiaro back-thrust appears to involve the Calabrian calcarenites that are exposed in the Montevago sector and may have dissected the terraces located at 400 m a.s.l of Mt. Magaggiaro area. These results, as a whole, show a dominant compressional strain that affected the mapped area and suggest that the leading basal thrust, at which the anticline and the backthrust are probably related, has been active during the Quaternary, at least until the Late Pleistocene. For these reasons, it is plausible that the thrust is still active and could be the seismic source of the 1968 destructive events.

### Software

The field survey of the geological observations was performed using a Dell Latitude XT2 Tablet-PC featured with an external small 51-channel Bluetooth GPS receiver and an SIRF antenna with the NMEA protocol and EGNOS correction. The georeferenced data were collected using Map-IT (De Donatis & Brucciatelli, 2006), a modified Shark GIS with a number of tools (GPS acquisition, Easy note, Form Editor, hand notes on maps and pictures, etc.). The data collected have been managed and stored in a georeferenced database using Esri ArcGIS. Adobe Illustrator CS6 was used for the final map production.

### Geolocation information

The study area is located in the lower Belice River valley, between the Poggio Reale and Menfi villages, in

the Trapani and Agrigento provinces, Southwestern Sicily, Italy.

## Acknowledgements

Field survey conducted in the framework of the Agreement INGV-DPC 2007-2009, Project S1 ‘Analysis of the seismic potential in Italy for the evaluation of the seismic hazard’, UR3.09 (Coordinated by Stefano Pucci). Digital cartographic elements of the Carta Tecnica Regionale 1:10.000-scale and shaded relief from LiDAR-derived digital elevation model (2 m/pixel resolution) by courtesy of Regione Siciliana.









## Disclosure statement

No potential conflict of interest was reported by the author(s).

## Data availability statement

The collected raw data were elaborated as project in ArcGIS environment at the INGV Geology and Geotechnology Laboratory (<https://www.ingv.it/it/monitoraggio-e-infrastrutture-per-la-ricerca/laboratori/laboratorio-geologia-e-geotecnologia>). This georeferenced data supporting the findings of this study are available from the corresponding author S. Pucci on request.

## ORCID

Stefano Pucci  <http://orcid.org/0000-0002-3557-2936>  
 Giuseppe Avellone  <http://orcid.org/0000-0002-7201-3420>  
 Antonio Contino  <http://orcid.org/0000-0003-4730-2869>  
 Alessandra Incarbona  <http://orcid.org/0000-0003-3563-7143>  
 Leonardo Sagnotti  <http://orcid.org/0000-0003-3944-201X>  
 Attilio Sulli  <http://orcid.org/0000-0002-7705-3632>  
 Enrico Di Stefano  <http://orcid.org/0000-0002-8102-5896>  
 Alessandra Smedile  <http://orcid.org/0000-0002-2938-4816>

## References

- Anderson, H., & Jackson, J. (1987). Active tectonics of the Adriatic region. *Geophysical Journal International*, 91(3), 937–983. <https://doi.org/10.1111/j.1365-246X.1987.tb01675.x>
- Arrowsmith, J. R., & Zielke, O. (2009). Tectonic geomorphology of the San Andreas Fault zone from high resolution topography: An example from the Cholame segment. *Geomorphology*, 113(1-2), 70–81. <https://doi.org/10.1016/j.geomorph.2009.01.002>
- Avellone, G., Barchi, M. R., Catalano, R., Morticelli, M. G., & Sulli, A. (2010). Interference between shallow and deep-seated structures in the Sicilian Fold and Thrust Belt, Italy. *Journal of the Geological Society*, 167(1), 109–126. <https://doi.org/10.1144/0016-76492008-163>
- Barbera, L. (1980). I ministri dal cielo: i contadini del Belice raccontano. Feltrinelli Ed., 190 pp.
- Barreca, G., Bruno, V., Cocorullo, C., Cultrera, F., Ferranti, L., Guglielmino, F., & Pepe, F. (2014). Geodetic and geological evidence of active tectonics in south-western Sicily (Italy). *Journal of Geodynamics*, 82, 138–149. <https://doi.org/10.1016/j.jog.2014.03.004>
- Basilone, L. (2012). *Litostratigrafia della Sicilia*. Arti Grafiche Palermitane s.r.l.
- Baumann, K. H., & Freitag, T. (2004). Pleistocene fluctuations in the northern Benguela current system as revealed by Coccolith assemblages. *Marine Micropaleontology*, 52(1-4), 195–215. <https://doi.org/10.1016/j.marmicro.2004.04.011>
- Bello, M., Franchino, A., & Merlini, S. (2000). Structural model of eastern Sicily. *Memorie della Società Geologica Italiana*, 55, 61–70.
- Bown, P. R., & Young, J. R. (1998). Techniques. In P. R. Bown (Ed.), *Calcareous nannofossil biostratigraphy* (pp. 16–28). Chapman and Hall.
- Cardamone, P., Casnedi, R., Cassinis, G., Cassinis, R., Marcolongo, B., & Tonelli, A. M. (1976). Study of regional linears in central Sicily by satellite imagery. *Tectonophysics*, 33(1-2), 81–96. [https://doi.org/10.1016/0040-1951\(76\)90052-4](https://doi.org/10.1016/0040-1951(76)90052-4)
- Catalano, R., Di Stefano, E., Sulli, A., Vitale, F. P., Infuso, S., & Vail, P. R. (1998). Sequences and systems tracts calibrated by high-resolution bio-chronostratigraphy: the central Mediterranean Plio-Pleistocene record. Mesozoic and Cenozoic Sequence Stratigraphy of European Basins, SEPM Special Publication No. 60 Copyright 1998, SEPM (Society for Sedimentary Geology), ISBN 1-56576-043-3.
- Catalano, R., Franchino, A., Merlini, S., & Sulli, A. (2000). Central western Sicily structural setting interpreted from seismic reflection profiles. *Memorie della Società Geologica Italiana*, 55, 5–16.
- Catalano, R., Valenti, V., Albanese, C., Accaino, F., Sulli, A., Tinivella, U., Gasparo Morticelli, M., Zanolla, C., & Giustiniani, M. (2013). Sicily’s fold/thrust belt and slab rollback: The S.I.R.I.PRO. Seismic crustal transect. *Journal of the Geological Society, London*, 170(3), 145. <https://doi.org/10.1144/jgs2012-099>
- D’Arpa, C., & Incarbona, A. (2022). Paleoenvironmental reconstruction on late Calabrian Stage sediments from the Belice Valley (Southwestern Sicily – Italy) based on Ostracoda. *Alpine and Mediterranean Quaternary*, 35(1), 69–83. <https://doi.org/10.26382/AMQ.2022.04>
- De Donatis, M., & Bruciatelli, L. (2006). MAP IT: The GIS software for field mapping with Tablet PC. *Computers & Geosciences*, 32(5), 673–680. <https://doi.org/10.1016/j.cageo.2005.09.003>
- Di Geronimo, I., Costa, B., La Perna, R., Randazzo, G., Rosso, A., & Sanfilippo, R. (1994). The Pleistocene ‘case Catarinichia’ section (Belice, SW Sicily). In R. Matteucci, M. G. Carboni, & J. S. Pignatti (Eds.), *Studies on ecology and paleoecology of benthic communities*, *Boll. Soc. Paleontol. It. Spec. Vol. 2, Mucchi, Modena* (pp. 93–115).
- Di Maggio, C., Agate, M., Contino, A., Basilone, L., & Catalano, R. (2009). Unità a limiti inconformi utilizzate per la cartografia dei depositi quaternari nei fogli CARG della Sicilia nord-occidentale. *Alpine and Mediterranean Quaternary*, 22(2), 345–364. <https://amq.aqua.it/index.php/amq/article/view/315>
- DISS Working Group. (2018). Database of Individual Seismogenic Sources (DISS), Version 3.2.1: A compilation of potential sources for earthquakes larger than M 5.5 in Italy and surrounding areas. <http://diss.rm.ingv.it/diss/>, Istituto Nazionale di Geofisica e Vulcanologia.
- Di Stefano, E., Caracausi, S., Incarbona, A., Ferraro, S., & Velardi, S. (2014). Size variations in the genus

- Gephyrocapsa during the Early Pleistocene in the eastern Mediterranean. *Italian Journal of Geosciences*, 133(3), 474–480. <https://doi.org/10.3301/IJG.2014.24>
- Di Stefano, E., Sprovieri, R., & Scarantino, S. (1991). Biostratigrafia e paleoecologia della sezione intrapleistocenica di Casa Parrino (Foce del Belice, Sicilia sud-occidentale). *Naturalista Siciliano*, 15(3–4), 115–148.
- Di Stefano, P., Renda, P., Zarccone, G., Nigro, F., Cacciatore, M., & Di Stefano, E. (2013). *Foglio 619, Santa Margherita di Belice*. SystemCart.
- Di Stefano, P., & Vitale, F. P. (1993). Carta Geologica della Valle del Belice in scala 1: 50.000. Lavori del Dipartimento di Geologia e Geodesia dell'Università di Palermo.
- Ferranti, L., Burrato, P., Sechi, D., Andreucci, S., Pepe, F., & Pascucci, V. (2021). Late Quaternary coastal uplift of southwestern Sicily, central Mediterranean sea. *Quaternary Science Reviews*, 255, 106812. <https://doi.org/10.1016/j.quascirev.2021.106812>
- Finetti, I. R., & Del Ben, A. (2005). Crustal tectono-stratigraphic setting of the Pelagian foreland from new CROP seismic data. In I. R. Finetti (Ed.), *Crop project: Deep seismic exploration of the central Mediterranean and Italy* (pp. 581–596). Elsevier.
- Fisher, R. A. (1953). Dispersion on a sphere. *Proceedings of the Royal Society London*, A217(1130), 295–305. <https://doi.org/10.1098/rspa.1953.0064>
- Flores, J.-A., Gersonde, R., Sierro, F. J., & Niebler, H.-S. (2000). Southern Ocean Pleistocene calcareous nannofossil events: Calibration with isotope and geomagnetic stratigraphies. *Marine Micropaleontology*, 40(4), 377–402. [https://doi.org/10.1016/S0377-8398\(00\)00047-5](https://doi.org/10.1016/S0377-8398(00)00047-5)
- Flores, J.-A., Marino, M., Sierro, F. J., Hodell, D. A., & Charles, C. D. (2003). Calcareous plankton dissolution pattern and coccolithophore assemblages during the last 600 kyr at ODP Site 1089 (Cape Basin, South Atlantic): Paleooceanographic implications. *Palaeogeography, Palaeoclimatology, Palaeoecology*, 196(3–4), 409–426. [https://doi.org/10.1016/S0031-0182\(03\)00467-X](https://doi.org/10.1016/S0031-0182(03)00467-X)
- Gasparini, C., Iannaccone, G., & Scarpa, R. (1985). Fault-plane solutions and seismicity of the Italian peninsula. *Tectonophysics*, 117(1–2), 59–78. [https://doi.org/10.1016/0040-1951\(85\)90236-7](https://doi.org/10.1016/0040-1951(85)90236-7)
- Goes, S., Giardini, D., Jenny, S., Hollenstein, C., Kahle, H.-G., & Geiger, A. (2004). A recent reorganization in the south-central Mediterranean. *Earth and Planetary Science Letters*, 226(3–4), 335–345. <https://doi.org/10.1016/j.epsl.2004.07.038>
- Gueguen, E., Doglioni, C., & Fernandez, M. (1998). On the post-25 Ma geodynamic evolution of the western Mediterranean. *Tectonophysics*, 298(1–3), 259–269. [https://doi.org/10.1016/S0040-1951\(98\)00189-9](https://doi.org/10.1016/S0040-1951(98)00189-9)
- Guidoboni, E., Ferrari, G., Tarabusi, G., Sgattoni, G., Comastri, A., Mariotti, D., Ciuccarelli, C., Bianchi, M. G., & Valensise, G. (2019). CFTI5Med, the new release of the catalogue of strong earthquakes in Italy and in the Mediterranean area. *Scientific Data*, 6(80), <https://doi.org/10.1038/s41597-019-0091-9>
- Guidoboni, E., Muggia, A., Marconi, C., & Boschi, E. (2002). A case study in archaeoseismology. The collapses of the Selinunte temples (Southwestern Sicily): Two earthquakes identified. *Bulletin of the Seismological Society of America*, 92(8), 2961–2982. <https://doi.org/10.1785/0120010286>
- Hine, N., & Weaver, P. P. E. (1998). Quaternary. In P. R. Bown (Ed.), *Calcareous nannofossil biostratigraphy* (pp. 266–283). Kluwer Academic Publishers.
- Incarbona, A., Di Stefano, E., & Bonomo, S. (2009). Calcareous nannofossil biostratigraphy of the Central Mediterranean Basin during the last 430 000 years. *Stratigraphy*, 6(1), 33–34.
- Lavecchia, G., Ferrarini, F., de Nardis, R., Visini, F., & Barbano, M. S. (2007). Active thrusting as a possible seismogenic source in Sicily (Southern Italy): Some insights from integrated structural–kinematic and seismological data. *Tectonophysics*, 445(3–4), 145–167. <https://doi.org/10.1016/j.tecto.2007.07.007>
- McKenzie, D. (1972). Active tectonics of the Mediterranean region. *Geophysical Journal International*, 30(2), 109–185. <https://doi.org/10.1111/j.1365-246X.1972.tb02351.x>
- Meletti, C., Marzocchi, W., D'Amico, V., Lanzano, G., Luzi, L., Martinelli, F., Pace, B., Rovida, A., Taroni, M., Visini, F., & Group, M. W. (2021). The new Italian seismic hazard model (MPS19). *Annals of Geophysics*, 64(1), SE112. <https://doi.org/10.4401/ag-8579>
- Meletti, C., Stucchi, M., Galadini, F., Leschiutta, I., & Scandone, P. (2000). Criteri e procedure per la compilazione di un inventario speditivo delle sorgenti potenziali di terremoti distruttivi finalizzato alla compilazione di una nuova mappa delle zone sismogenetiche per l'area italiana. Le ricerche del GNDT nel campo della pericolosità sismica (1996–1999). CNR-Gruppo Nazionale per la Difesa dai Terremoti-Roma, 379–397.
- Michetti, A. M., Brunamonte, F., & Serva, L. (1995). Paleoseismological evidence in the epicentral area of the January 1968 earthquakes, Belice, Southwestern Sicily. In *Bulletin of the Association of Engineering Geologists*, Spec. Pub. 6 “Perspectives in Paleoseismology” (pp. 127–139). Peanut Butter Publishing.
- Monaco, C., Mazzoli, S., & Tortorici, L. (1996). Active thrust tectonics in western Sicily (southern Italy): The 1968 Belice earthquake sequence. *Terra Nova*, 8(4), 372–381. <https://doi.org/10.1111/j.1365-3121.1996.tb00570.x>
- Orecchio, B., Scolaro, S., Batlló, J., Neri, G., Presti, D., Stich, D., & Totaro, C. (2021). New results for the 1968 Belice, South Italy, seismic sequence: Solving the long-lasting ambiguity on causative source. *Seismological Research Letters*, 92(4), 2364–2381. <https://doi.org/10.1785/0220200277>
- Ortolani, F., & Pagliuca, S. (1995). Evidenze geo-archeologiche di desertificazione ciclica nella zona di Selinunte (Sicilia sud-occidentale) in relazione alle variazioni climatiche dell'area mediterranea. 1° Convegno del Gruppo Naz. di Geol. Appl. “La città, fragile in Italia”, Giardini Naxos, 11–15 giugno 1995.
- Rio, D. (1982). The fossil distribution of Coccolithophore Genus Gephyrocapsa Kamptner and related Plio-Pleistocene chronostratigraphic problems. In W. L. Prell, & J. V. Gardner (Eds.), *Initial reports of the deep sea drilling project, v. 68* (pp. 325–343). U.S. Govt. Printing Office. <http://doi.org/10.2973/dsdp.proc.68.109.1982>
- Rio, D., Raffi, I., & Villa, G. (1990). Pliocene-Pleistocene calcareous nannofossil distribution patterns in the Western Mediterranean. In K. A. Kastens, & J. Masche (Eds.), *Proc. ODP Sc. Result.* (pp. 513–532). Ocean Drilling Program.
- Rovida, A., Locati, M., Camassi, R., Lolli, B., & Gasperini, P. (2020). The Italian earthquake catalogue CPTI15. *Bulletin of Earthquake Engineering*, 18, 2953–2984. <https://doi.org/10.1007/s10518-020-00818-y>
- Ruggieri, G., Rio, D., & Sprovieri, R. (1984). Remarks on the chronostratigraphic classification of Lower Pleistocene. *Bollettino Della Società Geologica Italiana*, 103(3), 251–259.

- Ruggieri, G., & Sprovieri, R. (1983). Recenti progressi nella stratigrafia del Pleistocene inferiore. *Bollettino Della Societa Paleontologica Italiana*, 22(3), 315–321.
- Ruggieri, G., & Unti, M. (1974). Pliocene e Pleistocene nell'entroterra di Marsala. *Bollettino Della Societa Geologica Italiana*, 93(3), 723–733.
- Sagnotti, L. (2013). Demagnetization Analysis in Excel (DAIE) – An open source workbook in excel for viewing and analyzing demagnetization data from paleomagnetic discrete samples and u-channels. *Annals of Geophysics*, 56(1), D0114. <https://doi.org/10.4401/ag-6282>
- Tondi, E., Zampieri, D., Giunta, G., Renda, P., Alessandrini, M., Unti, M., & Cello, G. (2006). Active faults and inferred seismic sources in the San Vito lo Capo peninsula, northwestern Sicily, Italy. *Geological Society, London, Special Publications*, 262(1), 365–377. <https://doi.org/10.1144/GSL.SP.2006.262.01.22>
- Villanueva, J., Flores, J. A., & Grimalt, J. O. (2002). A detailed comparison of the UK 37 and Coccolith records over the past 290 K Years: Implications to the Alkenone Paleotemperature method. *Organic Geochemistry*, 33(8), 897–905. [https://doi.org/10.1016/S0146-6380\(02\)00067-0](https://doi.org/10.1016/S0146-6380(02)00067-0)
- Vitale, F. P. (1995). Il segmento sicano della Catena Sud Tirrenica: bacini neogenici e deformazione attiva. Studi Geologici Camerti, “Geodinamica e tettonica attiva del sistema Tirreno-Appennino”, numero speciale, 1995/2 (pp. 491–507).
- Vitale, F. P., & Sulli, A. (1997, June 7–13). The regional pattern of the Belice and Menfi basins: A deep geologic profile. In R. Catalano (Ed.), 8° workshop ILP task force. “origin of sedimentary basins”, field workshop in Western Sicily, Guidebook, Altavilla Milicia (Palermo) (pp. 47–69). University of Palermo.
- Wagner, S., Costantini, E. A. C., Sauer, D., & Stahr, K. (2007). Soil genesis in a marine terrace sequence of Sicily, Italy. *Revista Mexicana de Ciencias Geológicas*, 24(2), 247–260.